Linear and Nonlinear Optical Properties of Ramified Hexaazatriphenylenes: Charge Transfer Contributions to the Octupolar Response

9 AUTHORS, INCLUDING:

Rafael Juárez
King Juan Carlos University
9 PUBLICATIONS **61** CITATIONS

José L Segura
Complutense University of Madrid
162 PUBLICATIONS **4,304** CITATIONS

Juan Teodomiro López Navarrete
University of Malaga
335 PUBLICATIONS **5,265** CITATIONS

Juan Casado
University of Malaga
227 PUBLICATIONS **3,690** CITATIONS

Linear and Nonlinear Optical Properties of Ramified Hexaazatriphenylenes: Charge Transfer Contributions to the Octupolar Response

María Moreno Oliva,[†] Rafael Juárez,[‡,§] Mar Ramos,[§] José L. Segura,*[,‡] Stijn van Cleuvenbergen,[‖] Koen Clays,[‖] Theodore Goodson, III,[⊥] Juan T. López Navarrete,*[,†] and Juan Casado*[,†]

[†]Department of Physical Chemistry, University of Málaga, Campus de Teatinos s/n, Málaga 29071, Spain
[‡]Department of Organic Chemistry, Faculty of Chemistry, Complutense University of Madrid, Madrid 28040, Spain
[§]Department of Environmental and Technological Chemistry, Universidad Rey Juan Carlos, Madrid 28933, Spain
[‖]Department of Chemistry, University of Leuven, Celestijnenlaan 200D, B-3001 Leuven, Belgium
[⊥]Department of Chemistry, University of Michigan, Ann Arbor, Michigan 48109, United States

Ⓢ Supporting Information

ABSTRACT: Four new HAT derivatives with octupolar symmetry have been synthesized. Their linear and nonlinear optical, photophysical, and electrochemical properties have been rationalized in terms of donor–acceptor interactions. We get further insights in the relationship between experimental first hyperpolarizability and two-photon absorption cross section: the δ/β ratio is connected with the electron donor–acceptor strength between the HAT core and the peripheral groups but also with the ethylene/acetylene bridges. This structure–property relationship can be used to design octupoles with more efficient nonlinear responses. A HAT derivative based on the fusion of three HAT cores and without any defined donor–acceptor pattern is studied in comparison with the charge transfer HAT versions. A complete study of the electronic structure of the five molecules in the context of the origin of the relevant optical properties is carried out combining several spectroscopic techniques and quantum chemistry.
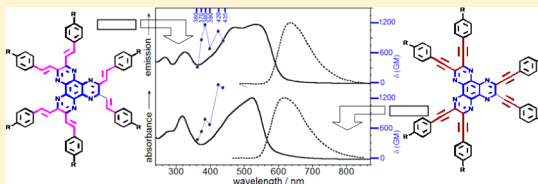
I. INTRODUCTION

HAT (Hexaazatriphenylene) can be regarded as an extended π-system where three pyrazine rings are fused to a central benzene core in an aromatic, disc-like moiety. Initially, HAT and its derivatives were employed as metal ligands in coordination chemistry.[1] More recently these platforms have been exploited in supramolecular chemistry taking advantage of noncovalent interactions such as π-stacking or van der Waals. Many interesting properties such as liquid crystalline behavior (they enabled the formation of robust nanorods and nanowires[2]),[3–5] field-effect electron mobilities,[6,7] nonlinear optics (NLO) responses,[8] self-assembling in surfaces[9,10] and in solution,[11,12] and theoretical studies[13,14] have deserved intensive research. In combination with other materials HAT samples have been used for color tuning in mesoporous silica materials[15] and implemented in OLED devices.[16,17] Most of these properties are based on the particular redox ability of HAT[18,19] to act as an electron acceptor group. The strong actual interest in organic molecular materials with two-photon absorption (TPA) properties (multiphotonic) to which octupolar dyes are great candidates and, in particular, HAT based systems must be highlighted.[20]

We decide here to further explore the electron-withdrawal property of HAT by ramifying and fully substituting its six peripheral positions with electron donor arms giving rise to

new octupolar extended HAT dyes (Figure 1) in a donor-to-acceptor pattern with modulation of the charge transfer character. In addition, it is interesting to compare the nonlinear optical behavior of charge transfer compounds **1–4** with that of a new HAT derivative, **tri-HAT**,[21] which consists of the fusion of three HAT molecules and that, without relying on donor–acceptor derived noncentrosymmetry (as necessitated in linear conjugated structures), epitomizes the purely octupolar implementation of noncentrosymmetry.

In this article, we propose a combination of spectroscopies (i.e., one-photon absorption, emission, and two-photon absorption) together with first hyperpolarizability properties and electrochemical analysis in conjunction with theoretical modeling in order to extract a picture of the relevant electro-optical phenomena that take place in these octupolar molecules and how these are modulated by the chemical structure. With regard to chemical design guidelines, we propose a comparison of the effect of the ramification of the HAT core with donor–acceptor arms with "charge transfer pattern" embedded in a octupolar symmetry with the effect of condensation of three
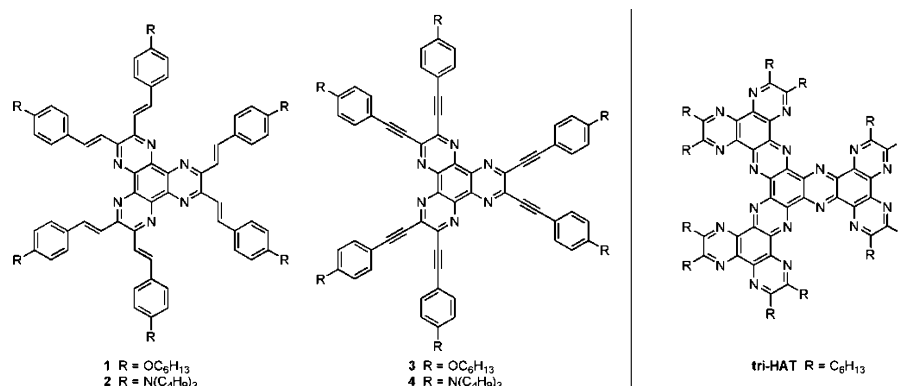
Figure 1. HAT derivatives synthesized in the present article and **tri-HAT**.[21]

HAT molecules which lacks "charge transfer patterns" and which we termed a pure "octupolar pattern".

II. EXPERIMENTAL AND THEORETICAL METHODOLOGIES

II.1. Synthesis. Analogous of **1** and **2** with shorter alkyl chains were previously reported, but reasonable synthetic yields could be obtained only by using high dilution conditions.[8] In that work, Cho et al. reported a nonlinear analysis of the β data for **1** and **2**. Here we have developed two different protocols for the synthesis of HAT derivatives **1**−**4** (Scheme 1, see more details in the Supporting Information), which allows us to include longer alkyl chains providing materials with greater solubility and processability without the need of using high dilution conditions.

Scheme 1. Synthesis Route Leading to the New HAT Derivatives
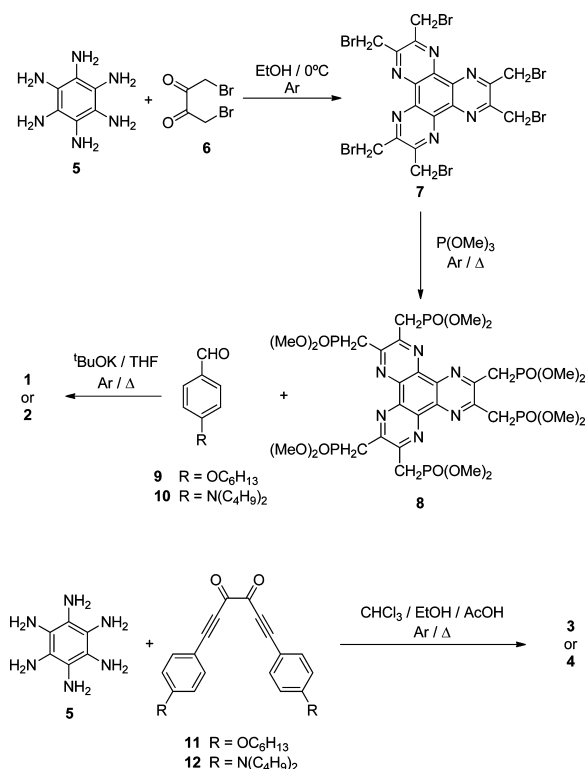
The first strategy requires the formation of a functionalized HAT derivative (**8**) which can be reacted through Wittig−Horner olefination reactions to afford the all-trans arylenevinylene-substituted HATs **1** and **2** with 80% and 32% yields, respectively. The synthesis of the hexabromomethylsubstituted HAT starts with the condensation of hexaaminobenzene (**5**) and 1,4-dibromobutanedione (**6**) to give the unstable intermediate **7**. The reaction of **7** with methyltriphosphite leads to phosphonate **8** as a versatile bulding block for the functionalization of HAT.

In the case of alkynyl linked HATs **3** and **4** the products are obtained by condensation of hexaaminobenzene (**5**) and the corresponding α-diketones (**11** or **12**) with 53% and 10% yields, respectively.

II.2. Spectroscopic and Electrochemical Measurements. UV−vis absorption spectra were recorded on an Agilent 8453 instrument equipped with a diode array detection system. Spectra deconvolution have been made with Peak Fit v.4.11 software. Emission spectra were measured using a spectrofluorometer from Edinburgh Analytical Instrument (FLS920P) equipped with a pulsed xenon flash-lamp. Fluorescence decays were measured by using a single photon photomultiplier detection system (S900) with picosecond pulsed diode laser (PDL 800-B), from Edinburgh Instruments. All solvents used were of spectroscopic grade from Aldrich. Fluorescence quantum yields, Φ_F, were measured for all the solutions using 1×10^{-7} mol L^{-1} quinine sulfate in 0.1 mol L^{-1} H$_2$SO$_4$ as the standard (Φ_F = 0.546). No fluorescent contaminants were detected upon excitation in the wavelength region of experimental interest. With this method fluorescent quantum yields of up to 0.001 can be accurately measured.

The two-photon excited fluorescence (TPEF) method was employed to evaluate the two-photon absorption cross sections (TPACS) of the samples.[22,23] The TPACS was evaluated over the excitation wavelength range of 710−900 nm using a mode-locked Ti:sapphire laser (Spectra-Physics MaiTai HP, pulse-width <100 fs, 80 MHz repetition rate). In applying the TPEF technique, two-photon absorption cross sections were measured relative to a reference solution of Rhodamine B (prepared at pH 10) in methanol at known concentration. TPACS for a specific excitation wavelength were evaluated at the emission wavelength corresponding to the maximum in the TPEF spectrum.

Electrochemical data were obtained with an Autolab PGSTAT 302. For working and counter electrodes Pt was used. Before each experiment the working electrode was submitted to the following cleaning procedure: Pt was polished
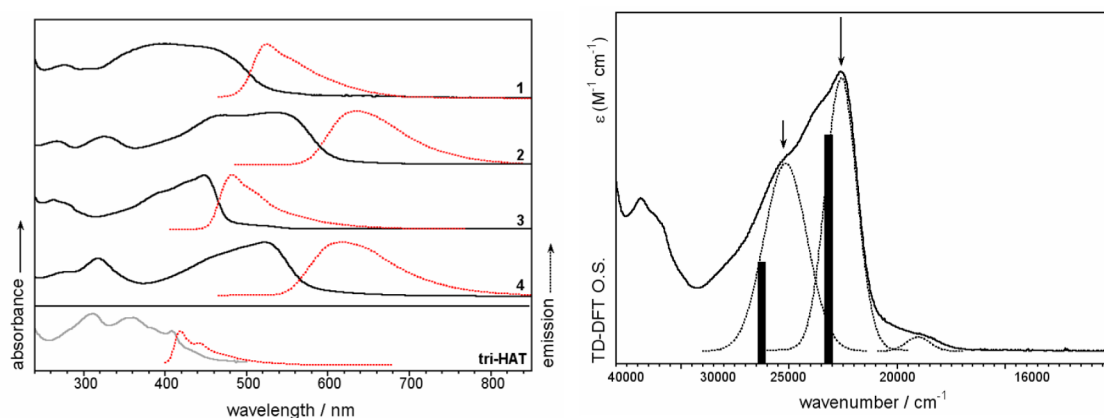
Figure 2. (Left) UV−vis spectra of **1**−**4** and **tri-HAT** together with their corresponding emission spectra in CH_2Cl_2. (Right) TD-DFT//B3LYP/6-31G** theoretical (bars) and experimental spectrum of **3** (in CH_2Cl_2) together with its deconvolution bands.
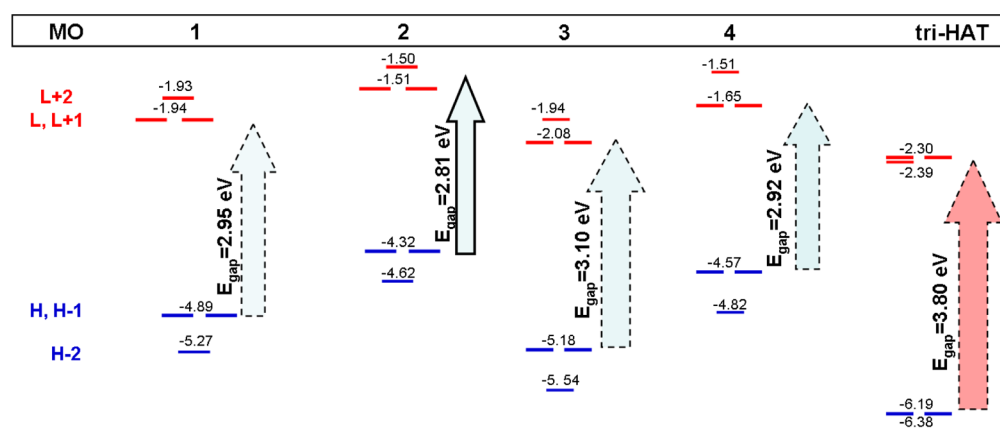

Figure 3. DFT//B3LYP/6-31G** molecular orbital energies of **1**−**4** and **tri-HAT**.

with fine emery paper followed by polishing with an alumina suspension over cloth and then ultrasonically cleaned in distilled water. A reference electrode, Ag/Ag⁺ (0.01 M AgNO₃ in acetonitrile) for nonaqueous solvent, was used in the electrochemical cell. The solvent employed was anhydrous and desoxygenated dichloromethane. The supporting electrolyte was tetrabutylammonium hexafluorophosphate (Aldrich, electrochemical grade). The voltammograms were obtained using a scan rate of 100 mV/s, and all of the values were referenced to the pair Fc/Fc⁺.

II.3. Nonlinear Optical Spectroscopy. Owing to the octupolar nature of the investigated compounds, hyper Rayleigh scattering (HRS) is the method of choice for determining the first hyperpolarizability β.[24] Here, frequency-resolved femtosecond HRS with fluorescence demodulation at 800 nm has been applied.[24] As a reference value, 330×10^{-30} esu was used for β_{xxx} of the octupolar molecule crystal violet in methanol, also at 800 nm.[24c] For both unknown and reference, the B-convention was adopted. Upon simultaneously fitting the demodulation and the phase data as a function of modulation frequency, the fluorescence-free hyperpolarizability values were obtained together with the multiphoton fluorescence contribution (MPF), and the fluorescence lifetime. The reported hyperpolarizability values are the dynamic, fluorescence-free values at 800 nm ($\beta_{xxx,800}$) and the static, dispersion-free values ($\beta_{xxx,0}$), as calculated using the two-level model.[24] See the Supporting Information for further details of the HRS measurements.

II.4. Theoretical Methods. The ground-state molecular geometries were calculated using Density Functional Theory (DFT) by means of the *Gaussian 03* programming package.[25] The Becke's three parameter (B3) gradient-corrected exchange functional combined with the correlation Lee−Yang−Parr (LYP) correlation functional was utilized.[26,27] The 6-31G** basis set was used.[28,29] The time-dependent DFT (TD-DFT) approach has been used for the evaluation of, at a minimum, the fifteen lowest-energy vertical electronic excited states.[30−32] The natural transition orbitals (NTOs)[33] were calculated by means of a formalism implemented in the *Gaussian 09* program suites,[25] taking TD-DFT as a starting point.

III. RESULTS AND DISCUSSION

III.1. Electronic Structure. The absorption spectra have been recorded in CH_2Cl_2 (Figure 2). The UV−vis spectra are characterized by the presence of bands of medium-high intensity in the range 390−550 nm. TD-DFT excited-state calculations helped us to assign the experimental bands. In the case of **3**, the lowest energy and strongest band at 448 nm corresponds to the double monoelectronic $S_0 \rightarrow S_5$ [HOMO → LUMO+2] and $S_0 \rightarrow S_6$ [HOMO-1 → LUMO+2] transitions predicted at $\lambda = 436$ nm. This band is followed at higher energies by a medium intensity band at $\lambda = 394$ nm due to the degenerate $S_0 \rightarrow S_{10}$ [HOMO-3 → LUMO] and $S_0 \rightarrow S_{11}$ [HOMO-3 → LUMO+1] excitations calculated at $\lambda = 374$ nm.

Table 1. Summary of Photophysical and Electrochemical (in Volts) Data in CH$_2$Cl$_2$ at 300 K

molecule	λ_{abs} [nm]	ε [M^{-1}cm^{-1}]	λ_F [nm]	Φ_F	$E_{red1}{}^a$	$E_{red2}{}^a$	$E_{red3}{}^a$	$E_{ox}{}^a$
1	452	38 750	525	0.022	−1.44	−1.70		+0.85
2	542	151 700	634	0.047	−1.34	−1.51	−1.80	+0.48
3	448	122 700	482	0.223	−1.15	−1.49		
4	524	146 600	620	0.031	−1.18	−1.53		+0.75

^{a}Conditions: concentrations of 2 mM of sample and 0.1 M of TBAPF$_6$ as supporting electrolyte; values referenced to Fc/Fc$^+$.
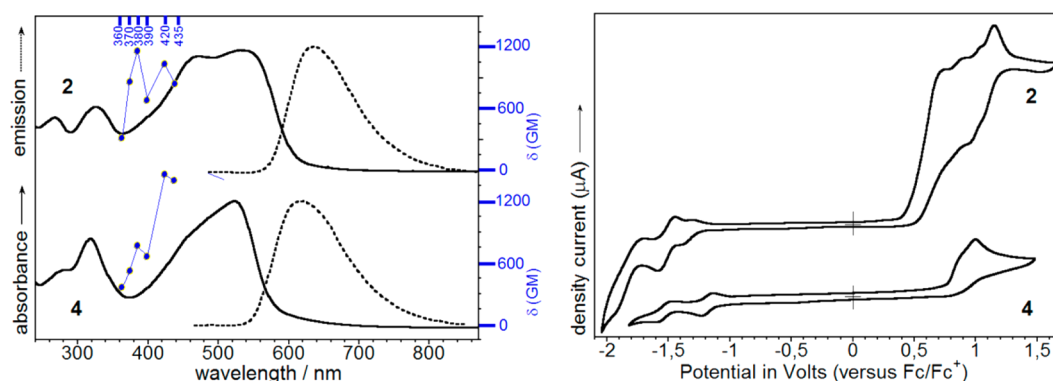

Figure 4. (Left) UV−vis (solid line), emission (dotted line), and TPA cross sections (blue line) spectra of **2** and **4** in CH$_2$Cl$_2$. (Right) Cyclic voltammetry waves of molecules **2** and **4** in CH$_2$Cl$_2$ with 0.1 M TBAPF$_6$.

In order to evaluate the accuracy of TD-DFT calculations, the experimental oscillator strength values (f_{exp}) of **3** were estimated by integrating the absorption bands, using the equation: $f_{exp} = (k/n) \int \varepsilon(\sigma)\, d\sigma$, where $\varepsilon(\sigma)$ is the molar extinction coefficient at wavenumber σ, n is the refractive index of the medium, and $k = 4.32 \times 10^{-9}$ M cm. The integrated absorption coefficient is found by determining the area under an absorption band that is displayed in Figure 2 as x axis = σ (cm^{-1}) against y axis = ε (M^{-1} cm^{-1}). In the case of **3**, a proper deconvolution of the main absorption band allowed us to identify its two contributions (448 and 394 nm) such as displayed in Figure 2. Experimental oscillator strength values (1.82 at 448 nm and 0.97 at 394 nm) are in reasonably good agreement with the theoretical oscillator strengths (1.82 at 436 nm and 0.80 at 374 nm). However, theoretically, the lowest lying energy transition is predicted at 464 nm with a zero oscillator strength which could be related with the absorption tail between 500 and 550 nm in the experimental spectrum with residual absorbance.

Going into more details of the electronic structure, it is interesting to study the diagram with the absolute energies of the frontier molecular orbitals (Figure 3; see the topologies in the Supporting Information). Given that the alkyl chains, in this case hexyl and butyl, do not contribute to the π-electron density of the molecular orbitals, they have been replaced by methyl groups in the theoretical calculations. Note that the HOMO/HOMO-1 and LUMO/LUMO+1 are degenerated. The description of the topologies in HOMO/HOMO-1 and LUMO/LUMO+1 is an electronic delocalization between the central core and different alternated arms, whereas the main contribution in HOMO-2 is located in the arms, with a small participation of the HAT core, centered in N atoms. In the case of LUMO+2, in the alkynyl derivatives, the electronic delocalization is particularly focused on the core and to a lesser extent in the acetylene bridge.

After replacing the triple by double bonds, there is a destabilization of the frontier orbitals, more marked in the case of HOMO/HOMO-1, resulting in a slight reduction of the band gap (3.10 eV in **3** → 2.95 eV in **1** and 2.89 eV in **4** → 2.81 eV in **2**). This behavior is consistent with the bathochromic shift observed in the absorption spectra (448 nm in **3** → 452 nm in **1** and 524 nm in **4** → 542 in **2**, Figure 2), indicating a favored scenario for conjugation in the alkenyl derivatives. Moreover, replacing the peripheral substituents −OC$_6$H$_{13}$ by −N(C$_4$H$_9$)$_2$ there is also a destabilization of HOMO/HOMO-1 and LUMO/LUMO+1, responsible for the reduction of the theoretical gap (2.95 eV in **1** → 2.81 eV in **2** and 3.10 eV in **3** → 2.89 eV in **4**), which also coincides with the bathochromic shift toward lower energies in the absorption bands (Figure 2), reflecting the greatest strength of the amine derivatives as electron donors.

It is interesting to compare compounds **1**−**4** with **tri-HAT**. Whereas the UV−vis spectra of the four substituted HAT derivatives have a main peak with an unresolved band around 390−550 nm, the UV−vis spectrum of **tri-HAT** shows three well-resolved maxima, blue-shifted bands (Figure 2). In Figure 3 it can be observed an important stabilization of the frontier orbitals (more marked in the case of occupied ones) of **tri-HAT**, leading to an increase of the gap, consistent with the shift toward higher energies in electronic spectra (Figure 2).

Table 1 summarizes the most relevant optical, cyclic voltammetry and photophysical data, whereas Figure 4 displays the spectra of some examples. The replacement of triple bonds by double bonds as spacers always leads to a red-shift of the absorption and emission maxima, a decrease of the fluorescence quantum yield, and lower oxidation potentials in consonance with the favorable conditions for π-conjugation by using C≡C spacers. Due to the HAT electron-withdrawing character, the four molecules display electron reduction processes, less energetic in the case of the acetylene derivatives owing to the larger electron deficiency of the sp versus the sp^2 carbon hybridization.

In general the optical spectra can be interpreted assuming a donor−acceptor interaction from the electron rich periphery to the central acceptor core with a partial modulation imparted by the unsaturated spacers. The charge transfer character resulting
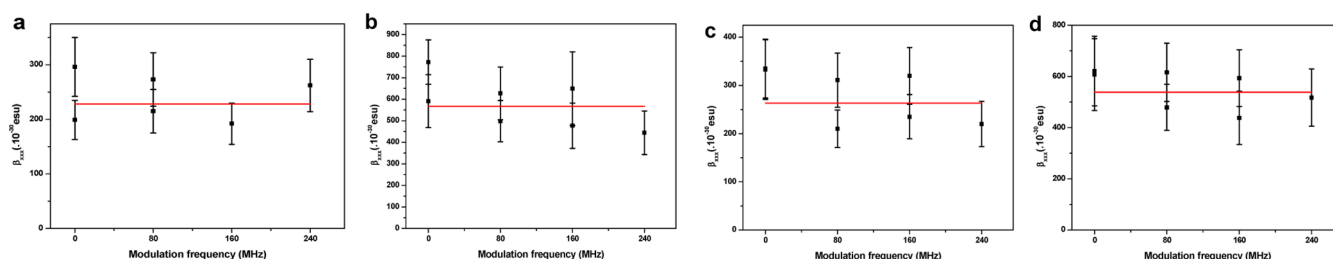
Figure 5. Hyper Rayleigh scattering of **1–4** (corresponding to a–d) at 800 nm for different modulation frequencies in two independently repeated experiments. The weighted average β_{xxx} value is depicted as a red line.

Table 2. Dynamic and Static First Hyperpolarizability Values,[36] HOMO-LUMO Theoretical Energy Gap, Experimental Optical Gap, Two-Photon Absorption Cross Sections at 840 nm in CH_2Cl_2, Theoretical Oscillator Strength, and Dipole Moment

molecule	$\beta_{xxx,800}$ [10^{-30} esu]	$\beta_{xxx,0}$ [10^{-30} esu]	$\Delta E_{H/L}$ [eV]	optical gap [eV]	δ_{840} [GM]	f	$|\Delta\mu_{12}|^e$ [D]
1	250 ± 50	50 ± 10	2.97	2.74	13 ± 6 (68)^c	1.21^a	4.14
2	550 ± 120	250 ± 50	2.79	2.29	850 ± 150 (1022)^c	1.24^a	5.68
3	290 ± 65	55 ± 10	3.11	2.77	120 ± 5 (888)^d	1.89^a	3.35
4	510 ± 110	220 ± 45	2.89	2.37	1300 ± 400	0.97^a	8.51
tri-HAT	690 ± 110	35 ± 5	3.80	3.03	-	0.5619^b	7.7461

^{a}Degenerate excited states S_5 and S_6. ^{b}Degenerate excited states S_{18} and S_{19}. ^{c}Absolute maximum at 760 nm. ^{d}Absolute maximum at 740 nm. ^{e}In a three-level model considering the ground electronic state, 0, and the double low-lying degenerated excited states, 1 and 2, $|\Delta\mu_{12}|$ defines the variation of the dipole moments between 1 and 2.

from this donor−acceptor coupling is evidenced in the rather broad aspect of the low energy bands of the optical spectra and in the low fluorescence activity.

In the negative electrochemical potential regime, only **2** exhibits the three quasireversible waves typical of the hexaazatriphenylene core[34] associated with the three pyrazine moieties of HAT. For **1**, **3**, and **4** (Table 1 and Figure S2), only the first two reduction waves are kinetically observable.

III.2. Nonlinear Optical Spectroscopy. In Figure 5 the experimental results of the HRS experiments are shown for **1–4**. Since low concentrations of the samples were used, the measurements were performed close to the molecular resonances keeping the absorption at the second harmonic wavelength low what limits the observed HRS response and the signal-to-noise ratio. Therefore these measurements were repeated independently. For all of the compounds, there were no multiphoton fluorescence contributions at this wavelength (i.e., 800 nm), and hence no demodulation of the β-values was observed. For **1–4**, this is in line with the more red-shifted one-photon fluorescence spectra.

Molecules with octupolar symmetry have been developed for nonlinear optical materials[35] taking advantage of the better transparency in the visible spectrum in comparison to dipolar push−pull dyes. The NLO properties of compounds **1–4** have been determined both by hyper Rayleigh scattering (HRS)[24] and by two-photon excitation fluorescence (TPEF),[22,23] and the main results are summarized in Table 2 (for more details see the Supporting Information, Figure S3 and Table S1).

The β values obtained for the alkoxy substituted molecules **1** and **3** are on the same order of magnitude as others previously reported for conjugated octupolar molecules with donor−acceptor substitution patterns.[37−39] A considerable enhancement of the dynamic and static first hyperpolarizability is observed however in molecules **2** and **4** with peripheral amine substitution. This can be explained in terms of the more efficient charge transfer interaction between the HAT core and the strong electron donating $-N(C_4H_9)_2$ groups, independ-

ently of the spacer and in consonance also with the HOMO−LUMO energy gap contraction imparted by this coupling.

To further complete the study of the NLO properties, we have measured two-photon absorption spectra. The representative values obtained for the TPA cross sections (δ) at 840 nm for each sample are shown in Table 2, whereas Figure 4 represents the variation of δ with the excitation wavelength for **2** and **4**. A considerable increase of δ values is observed by replacing $-OC_6H_{13}$ by $-N(C_4H_9)_2$ at this wavelength highlighting the close connection between charge transfer extension and the TPA response. Modest values are measured for alkoxy derivatives. A significant enhancement of δ is also recorded by inserting acetylene instead of ethylene spacers likely expressing the additive effect in the electron withdrawal effect of two acceptors acting in the same direction from the periphery to the central site. Only at shorter excitation wavelengths (i.e., close to 700 nm), the correlation between the δ values and the charge transfer character is not straightforward among compounds **1−4** suggesting that the measure of δ by the TPEF method might have interfering effects. In this study, the increase of δ values is consistent with the rise of β values and with the decrease of the experimental optical and theoretical HOMO−LUMO gaps (Table 2): Molecules **2** and **4** present the highest values of δ/β and the lowest ΔE_{H-L} and optical gaps.

We have conducted theoretical calculations of the excited states of the five samples (see ESI for further details, Tables S2−S6) and obtained the oscillators strength and the variation of the dipole moments along the most relevant electronic excitations contributing to the nonlinear response. These data are summarized in Table 2. We observed that compound **4**, which has the largest nonlinear responses (β and δ), also shows the largest $|\Delta\mu_{12}|$ value revealing the contribution of charge transfer character to the octupolar response. This effect also gives account of the enhancement of the signal with the substitution of $-OC_6H_{13}$ by $-N(C_4H_9)_2$ groups further underlining the electron donor ability of amines.
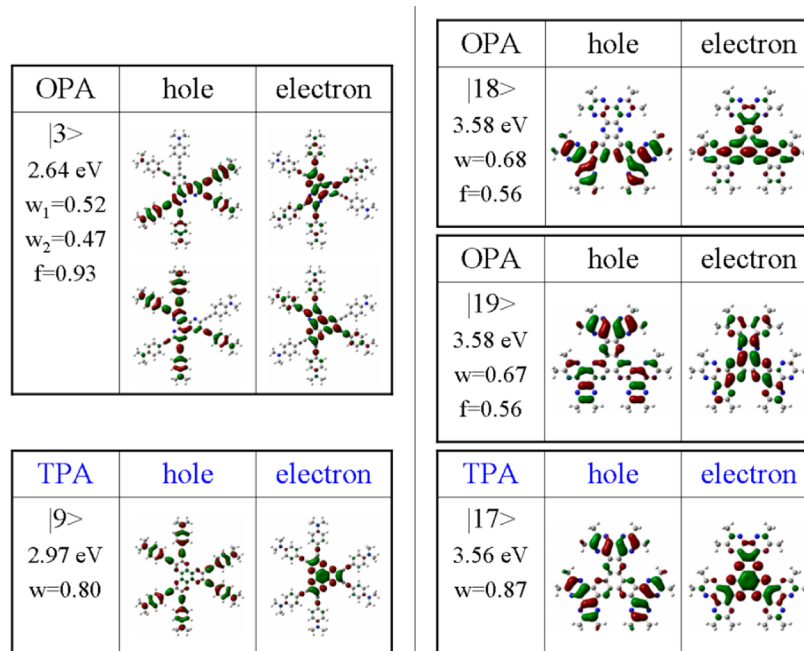
Figure 6. Natural transition orbitals describing the OPA and TPA states for molecule **4** (left) and **tri-HAT** (right). The corresponding excited-state number, its excitation energy in eV, the fraction of the NTO pair contribution into the given electronic excitation (w), and oscillator strength for the OPA excitations are indicated. In the case when the NTO fraction is less than 0.65, two NTO pairs are plotted.

The β values for **tri-HAT** (Table 2) have been also measured. Surprisingly it displays a rather strong HRS static signal comparable to those of **1** and **3** (note that for **tri-HAT** the dynamic β value is strongly resonantly enhanced due to the proximity of the absorption resonance wavelength to the second-harmonic wavelength). This large β value seems surprisingly high since **tri-HAT** does not follow a typical donor–acceptor paradigm. Recently, some of us have shown that octupolar symmetry by itself, realized by four non charge transfer moieties in a tetrahedral arrangement,[40,41] also results in a large second-order β nonlinear response. **tri-HAT** seems to be a new example of dye with a large second-order response, in origin derived from its octupolar symmetry, but in amplitude not relying on charge-transfer contributions between donor and acceptor substituents on the octupolar core, as in molecules **1**–**4**.

To further analyze the nature of the excited states involved in the linear and nonlinear responses, natural transition orbital (NTO)[33] analysis have been performed for molecule **4** and **tri-HAT** (Figure 6). NTOs offer the most compact representation of a given multielectron transition in terms of an expansion into single-particle transitions.[42] The NTOs associated with the one-photon absorption (OPA) excited states of lowest energy in **4** and **tri-HAT** reveal a localization of the excited-state density over the HAT core and over particular arms due to the energy degeneracy of these frontier molecular orbitals in both molecules. However, NTOs for the selected excited states contributing to the TPA response in **4** and **tri-HAT** show delocalized character of the electron and/or hole orbitals and a largely pronounced charge-transfer character from the moieties at the periphery to the HAT with a nice octupolar paradigm. Both molecules present similar NTOs associated with the TPA response, especially in electron orbitals, localized in the common HAT core. Going into more quantitative analysis, **tri-HAT** also exhibits a great $|\Delta\mu_{12}|$ comparable to that of **4** accompanied by a considerably lower oscillator strength which

would justify its lower β static value. It turns out that, in despite of its pure octupolar symmetry, **tri-HAT** would retain a slight charge transfer character which could be viewed as the central HAT acting as the electron acceptor with respect to the outermost electron donor rings.

IV. CONCLUSIONS

We have synthesized four new molecules comprising a central HAT core substituted by six alkenyl or alkynyl arms, with different electron donor groups in the periphery and different spacers. These compounds present relevant optical and NLO properties which are modulated by charge transfer interactions. The amine derivatives turn out to exalt the NLO activity due to their large electron donor capacity. The second order response of the HAT derivatives with charge transfer contributions have been compared with that of an inherently octupolar HAT derivative, **tri-HAT**, which also displays significant β values. In this regard, this comparison reveals (i) the modulation of the second order optical response by the balance of charge transfer and octupolar contributions with **tri-HAT** possibly taking from both mechanisms; (ii) chemical design to tune nonlinear properties. These are interesting insights and features that can guide the investigation of novel materials with new opto-electronic applications. Furthermore, the linear relationship between β and δ can be a useful guide for developing new strategies to synthesize compounds with great NLO and TPA properties.

■ ASSOCIATED CONTENT

⑤ Supporting Information

Detailed methods of the synthesis of HAT derivatives, HRS measurements, molecular orbital energies and topologies of **1**, complete data of cyclic voltammetry waves, absorption and emission spectra, TPA cross sections, and TD-DFT calculations. This material is available free of charge via the Internet at http://pubs.acs.org.

AUTHOR INFORMATION

Corresponding Author
*E-mail: casado@uma.es.

Notes
The authors declare no competing financial interest.

REFERENCES

(1) Nasielski-Hinkens, R.; Benedek-Vamos, M.; Maetens, D.; Nasielski, J. *J. Organomet. Chem.* **1981**, *217*, 179−182.

(2) Yip, H.-L.; Zou, J.; Ma, H.; Tian, Y.; Tucker, N. M.; Jen, A. K.-Y. *J. Am. Chem. Soc.* **2006**, *128*, 13042−13043.

(3) Ong, C. W.; Liao, S.-C.; Chang, T. H.; Hsu, H.-F. *J. Org. Chem.* **2004**, *69*, 3181−3185.

(4) Boden, N.; Bushby, R. J.; Cooke, G.; Lozman, O. R.; Lu, Z. *J. Am. Chem. Soc.* **2001**, *123*, 7915−7916.

(5) Arikainen, E. O.; Boden, N.; Bushby, R. J.; Lozman, O. R.; Vinter, J. G.; Wood, A. *Angew. Chem., Int. Ed.* **2000**, *39*, 2333−2336.

(6) Kaafarani, B. R.; Kondo, T.; Yu, J.; Zhang, Q.; Dattilo, D.; Risko, C.; Jones, S. C.; Barlow, S.; Domercq, B.; Amy, F.; et al. *J. Am. Chem. Soc.* **2005**, *127*, 16358−16359.

(7) Chan, C. K.; Amy, F.; Zhang, Q.; Barlow, S.; Marder, S.; Kahn, A. *Chem. Phys. Lett.* **2006**, *431*, 67−71.

(8) Cho, B. R.; Lee, S. K.; Kim, K. A.; Son, K. N.; Kang, T. I.; Jeon, S. J. *Tetrahedron Lett.* **1998**, *39*, 9205−9208.

(9) Salomon, E.; Zhang, Q.; Barlow, S.; Marder, S. R.; Kahn, A. *J. Phys. Chem. C* **2008**, *112*, 9803−9807.

(10) Ha, S. D.; Zhang, Q.; Barlow, S.; Marder, S. R.; Kahn, A. *Phys. Rev. B* **2008**, *77*, 085433(1)−085433(7).

(11) Ishi-i, T.; Yaguma, K.; Kuwahara, R.; Taguri, Y.; Mataka, S. *Org. Lett.* **2006**, *8*, 585−588.

(12) Ishi-i, T.; Murakami, K.-i.; Imai, Y.; Mataka, S. *J. Org. Chem.* **2006**, *71*, 5752−5760.

(13) Lemaur, V.; da Silva Filho, D. A.; Coropceanu, V.; Lehmann, M.; Geerts, Y.; Piris, J.; Debije, M. G.; van de Craats, A. M.; Senthilkumar, K.; Siebbeles, L. D. A.; et al. *J. Am. Chem. Soc.* **2004**, *126*, 3271−3279.

(14) Lozman, O. R.; Bushby, R. J.; Vinter, J. G. *J. Chem. Soc., Perkin Trans. 2* **2001**, 1446−1452.

(15) Okabe, A.; Fukushima, T.; Ariga, K.; Aida, T. *Angew. Chem., Int. Ed.* **2002**, *41*, 3414−3417.

(16) Liao, L.-S.; Slusarek, W. K.; Hatwar, T. K.; Ricks, M. L.; Comfort, D. L. *Adv. Mater.* **2008**, *20*, 324−329.

(17) Liao, L. S.; Klubek, K. P. *Appl. Phys. Lett.* **2008**, *92*, 223311(1)−223311(3).

(18) Furukawa, S.; Okubo, T.; Masaoka, S.; Tanaka, D.; Chang, H.-C.; Kitagawa, S. *Angew. Chem., Int. Ed.* **2005**, *44*, 2700−2704.

(19) Wang, R.; Okajima, T.; Kitamura, F.; Matsumoto, N.; Thiemann, T.; Mataka, S.; Ohsaka, T. *J. Phys. Chem. B* **2003**, *107*, 9452−9458.

(20) Beljonne, D.; Wenseleers, W.; Zojer, E.; Shuai, Z.; Vogel, H.; Pond, S. J. K.; Perry, J. W.; Marder, S. R.; Brédas, J.-L. *Adv. Funct. Mater.* **2002**, *12*, 631−641.

(21) Juárez, R.; Moreno Oliva, M.; Ramos, M.; Segura, J. L.; Alemán, C.; Rodríguez-Ropero, F.; Curcó, D.; Montilla, F.; Coropceanu, V.; Brédas, J.-L. *Chem.—Eur. J.* **2011**, *17*, 10312−10322.

(22) Xu, C.; Webb, W. W. *J. Opt. Soc. Am. B* **1996**, *13*, 481−491.

(23) Makarov, N. S.; Drobizhev, M.; Rebane, A. *Opt. Express* **2008**, *16*, 4029−4047.

(24) (a) Clays, K.; Wostyn, K.; Persoons, A. *Adv. Funct. Mater.* **2002**, *12*, 557−563. (b) Hendrickx, E.; Clays, K.; Persoons, A. *Acc. Chem. Res.* **1998**, *31*, 675−683. (c) Olbrechts, G.; Strobbe, R.; Clays, K.; Persoons, A. *Rev. Sci. Instrum.* **1998**, *69*, 2233−2241. (d) Wostyn, K.; Binnemans, K.; Clays, K.; Persoons, A. *Rev. Sci. Instrum.* **2001**, *72*, 3215−3220.

(25) Frisch, M. J.; Trucks, G. W.; Schlegel, H. B.; Scuseria, G. E.; Robb, M. A.; Cheeseman, J. R.; Montgomery, Jr., J. A.; Vreven, T.; Kudin, K. N.; Burant, J. C. et al. *Gaussian 03*, revision D.02; Gaussian, Inc.: Wallingford, CT, 2004.

(26) Lee, C.; Yang, W.; Parr, R. G. *Phys. Rev. B* **1988**, *37*, 785−789.

(27) Becke, A. D. *J. Chem. Phys.* **1993**, *98*, 5648−5652.

(28) Hehre, W. J.; Ditchfield, R.; Pople, J. A. *J. Chem. Phys.* **1972**, *56*, 2257−2261.

(29) Francl, M. M.; Pietro, W. J.; Hehre, W. J.; Binkley, J. S.; Gordon, M. S.; DeFrees, D. J.; Pople, J. A. *J. Chem. Phys.* **1982**, *77*, 3654−3665.

(30) Runge, E.; Gross, E. K. U. *Phys. Rev. Lett.* **1984**, *52*, 997−1000.

(31) Gross, E. K. U.; Kohn, W. *Adv. Quantum Chem.* **1990**, *21*, 255−291.

(32) Heinze, H. H.; Görling, A.; Rösch, N. *J. Chem. Phys.* **2000**, *113*, 2088−2099.

(33) Martin, R. L. *J. Chem. Phys.* **2003**, *118*, 4775−4777.

(34) Jia, C.; Liu, S.-X.; Tanner, C.; Leiggener, C.; Sanguinet, L.; Levillain, E.; Leutwyler, S.; Hauser, A.; Decurtins, S. *Chem. Commun.* **2006**, 1878−1880.

(35) (a) Ledoux, I.; Zyss, J.; Siegel, J. S.; Brienne, J.; Lehn, J.-M. *Chem. Phys. Lett.* **1990**, *172*, 440−444. (b) Zyss, J.; Ledoux, I. *Chem. Rev.* **1994**, *94*, 77−105.

(36) Joffre, M.; Yaron, D.; Silbey, R. J.; Zyss, J. *J. Chem. Phys.* **1992**, *97*, 5607−5615.

(37) (a) Hennrich, G.; Asselberghs, I.; Clays, K.; Persoons, A. *J. Org. Chem.* **2004**, *69*, 5077−5081. (b) Moreno Oliva, M.; Casado, J.; Hennrich, G.; López Navarrete, J. T. *J. Phys. Chem. B* **2006**, *110*, 19198−19206. (c) Moreno Oliva, M.; Hennrich, G.; Casado, J.; López Navarrete, J. T. *J. Mol. Struct.* **2007**, *834−836*, 369−373.

(38) (a) Asselberghs, I.; Hennrich, G.; Clays, K. *J. Phys. Chem. A* **2006**, *110*, 6271−6275. (b) Moreno Oliva, M.; Casado, J.; López Navarrete, J. T.; Hennrich, G.; Ruiz Delgado, M. C.; Orduna, J. *J. Phys. Chem. C* **2007**, *111*, 18778−18784. (c) Ruiz Delgado, M. C.; Orduna, J.; Moreno Oliva, M.; Casado, J.; López Navarrete, J. T. *J. Chem. Phys.* **2007**, *127*, 164704(1)−164704(6).

(39) Moreno Oliva, M.; Casado, J.; López Navarrete, J. T.; Hennrich, G.; van Cleuvenbergen, S.; Asselberghs, I.; Clays, K.; Ruiz Delgado, M. C.; Brédas, J.-L.; Seixas de Melo, J. S.; et al. *Chem.—Eur. J.* **2009**, *15*, 8223−8234.

(40) Quintiliani, M.; Pérez-Moreno, J.; Asselberghs, I.; Vázquez, P.; Clays, K.; Torres, T. *J. Phys. Chem. B* **2010**, *114*, 6309−6315.

(41) Van Cleuvenbergen, S.; Asselberghs, I.; García-Frutos, E. M.; Gómez-Lor, B.; Clays, K.; Pérez-Moreno, J. *J. Phys. Chem. C* **2012**, *116*, 12312−12321.

(42) Badaeva, E.; Harpham, M. R.; Guda, R.; Süzer, Ö.; Ma, C.-Q.; Bäuerle, P.; Goodson, T., III; Tretiak, S. *J. Phys. Chem. B* **2010**, *114*, 15808−15817.

632

dx.doi.org/10.1021/jp307563u | *J. Phys. Chem. C* 2013, 117, 626−632